

Polymorphism in a secondary phosphine

Mo Liu, Keith Izod and Paul G. Waddell*

School of Natural and Environmental Sciences, Bedson Building, Newcastle University, Newcastle upon Tyne, NE1 7RU, United Kingdom. *Correspondence e-mail: paul.waddell@ncl.ac.uk

Received 10 December 2024

Accepted 21 January 2025

Edited by T. Ohhara, J-PARC Center, Japan Atomic Energy Agency, Japan

Keywords: crystal structure; secondary phosphine; polymorphism; crystal packing; Me... π interactions; steric pressure.

CCDC references: 2405774; 2405773

Supporting information: this article has supporting information at journals.iucr.org/c

Two crystal structures of bis(2,3,5,6-tetramethylphenyl)phosphine, $C_{20}H_{27}P$, are reported constituting the first recorded case of polymorphism in a secondary phosphine (R_2PH). The two structures differ in their conformation and, as a result, the steric hindrance experienced at the phosphorus centre is observed to be dependent on the packing environment. Each polymorph exhibits a distinct supramolecular structure; in polymorph **I** the molecules are arranged in columns in two directions, whereas polymorph **II** forms layers. There is a distinct lack of significant intermolecular interactions in either form, with the exception of some weak Me... π interactions observed in polymorph **II**. These interactions are likely the cause of the variation in the C—P—C angles observed between the two structures.

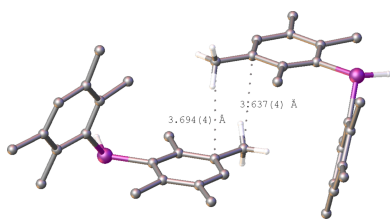
1. Introduction

Phosphines have become ubiquitous ligands for transition-metal centres due to the ease with which their electronic and steric properties may be tailored and to the many and varied applications of transition-metal phosphine complexes in catalysis. Secondary phosphines R_2PH have the added advantage that the P—H proton may readily be removed to furnish anionic phosphanide R_2P^- ligands (Izod, 2000). We have a long-standing interest in the application of such phosphanide ligands for the support of novel low-oxidation-state main group species; for example, the recently isolated fully phosphanyl-substituted ditetrelenes $\{(Mes)_2P\}_2E=E\{P(Mes)_2\}_2$ ($E = Si$ or Ge ; $Mes = 2,4,6-Me_3C_6H_2$) (Izod *et al.*, 2017a, 2022).

In the course of this work, we have striven to explore the impact of the steric profile and substitution pattern of the aromatic rings in diarylphosphanide ligands on the structures and stabilities of both low-oxidation-state main group compounds and their alkali metal precursors R_2PM ($M = Li, Na$ or K) (Izod *et al.*, 2017b). While 2,6-disubstituted and 2,4,6-trisubstituted aromatic rings are common phosphine substituents, alternative substitution patterns, such as in the 2,3,5,6-tetramethylphenyl substituent described here, are rare.

Due to their reactivity, the structure determination of secondary phosphines using single-crystal X-ray crystallography can be challenging, with the first such structure being reported in 1987 (Bartlett *et al.*, 1987). As testament to this, at time of writing there are only 95 organic acyclic secondary phosphine structures in the Cambridge Structural Database (CSD, Version 5.45, update 2, June 2024; Groom *et al.*, 2016) and only one polymorph is reported for any one secondary phosphine compound, including cyclic phosphines and organometallic complexes.

In this work, we present the first known instance of polymorphism in a secondary phosphine. Bis(2,3,5,6-tetramethylphenyl)phosphine (Fig. 1) crystallizes in two distinct forms:



Published under a CC BY 4.0 licence

Table 1

Experimental details.

For both structures: $C_{20}H_{27}P$, $M_r = 298.38$. Experiments were carried out at 150 K with Cu $K\alpha$ radiation using a Rigaku Xcalibur Gemini ultra diffractometer with an Atlas detector. The absorption correction was analytical [*CrysAlis PRO* (Rigaku OD, 2015), based on expressions derived by Clark & Reid (1995)]. H atoms were treated by a mixture of independent and constrained refinement.

	Polymorph I	Polymorph II
Crystal data		
Crystal system, space group	Monoclinic, $P2_1/n$	Monoclinic, $P2_1/c$
a, b, c (Å)	6.5476 (2), 5.9910 (2), 21.5676 (6)	12.8874 (6), 8.8455 (3), 15.4635 (7)
β (°)	96.020 (2)	104.108 (5)
V (Å ³)	841.36 (4)	1709.61 (13)
Z	2	4
μ (mm ⁻¹)	1.35	1.33
Crystal size (mm)	0.24 × 0.08 × 0.06	0.36 × 0.14 × 0.05
Data collection		
T_{\min}, T_{\max}	0.696, 0.866	0.746, 0.939
No. of measured, independent and observed [$I > 2\sigma(I)$] reflections	11409, 1500, 1299	12709, 3021, 2424
R_{int}	0.040	0.039
$(\sin \theta/\lambda)_{\text{max}}$ (Å ⁻¹)	0.596	0.596
Refinement		
$R[F^2 > 2\sigma(F^2)], wR(F^2), S$	0.039, 0.118, 1.06	0.047, 0.135, 1.06
No. of reflections	1500	3021
No. of parameters	103	214
No. of restraints	0	182
$\Delta\rho_{\text{max}}, \Delta\rho_{\text{min}}$ (e Å ⁻³)	0.27, -0.24	0.43, -0.35

Computer programs: *CrysAlis PRO* (Rigaku OD, 2015), *SHELXT* (Sheldrick, 2015a), *SHELXL* (Sheldrick, 2015b) and *OLEX2* (Dolomanov *et al.*, 2009).

polymorph **I**, grown from tetrahydrofuran, which crystallizes in the monoclinic space group $P2_1/n$, and polymorph **II**, grown from fluorobenzene, which crystallizes in the monoclinic space group $P2_1/c$. As the first case of its kind, the structural analysis here should provide unique insights into the supramolecular chemistry of secondary phosphines.

2. Experimental

2.1. Preparation of bis(2,3,5,6-tetramethylphenyl)phosphine

All manipulations were performed under an inert atmosphere (argon gas) using standard Schlenk techniques unless otherwise stated. To a cold (-78°C) solution of PCl_3 (2.9 ml, 23 mmol) in diethyl ether (50 ml) was added (2,3,5,6-Me₄-C₆H)₂MgBr (42 mmol) dissolved in tetrahydrofuran (THF, 200 ml). This mixture was allowed to warm to room temperature and was stirred for 12 h. To this solution was carefully added an excess of solid LiAlH_4 (1.0 g, 26.3 mmol) and the resulting mixture was stirred at room temperature for 2 h. Degassed water (50 ml) was carefully added and the organic

phase was extracted into THF (3 × 30 ml). The combined organic extracts were dried over activated 4 Å molecular sieves, the solution was filtered and solvent was removed *in vacuo* from the filtrate to give bis(2,3,5,6-tetramethylphenyl)phosphine as a colourless solid in 65% yield. Crystals suitable for single-crystal X-ray diffraction were grown from cold (3°C) THF (polymorph **I**) or from cold (-30°C) fluorobenzene (polymorph **II**).

2.2. Refinement

Crystal data, data collection and structure refinement details are summarized in Table 1. H atoms bound to C atoms were positioned with idealized geometry. The displacement parameters of these H atoms were constrained using a riding model, with $U_{\text{iso}}(\text{H})$ values set to be an appropriate multiple of the U_{eq} value of the parent atom.

The H atoms bound to phosphorus were located using peaks in the Fourier difference map. In both structures, the most prominent residual peaks about phosphorus after all other atoms were modelled were selected. In the case of polymorph **I**, the occupancy of this H atom was constrained to be 0.5 as it is disordered across a special position. For polymorph **II**, peaks corresponding to two proton positions with similar geometry were observed and hence the phosphine H atom was split across two positions with the occupancies refined to be approximately 63 and 37%. The displacement parameters of the phosphine H atoms in both structures were constrained using a riding model, with $U_{\text{iso}}(\text{H})$ values set to be $1.2U_{\text{eq}}$ relative to the parent atom.

It is likely that the unrestrained P–H distances are shorter than the true bond lengths, but the direction of the bond

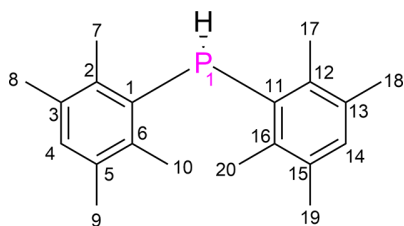


Figure 1

Bis(2,3,5,6-tetramethylphenyl)phosphine with the numbering scheme used in this article.

Table 2
Selected geometric parameters (\AA , $^\circ$) for polymorphs **I** and **II**.

	Polymorph I	Polymorph II
P1—C1	1.8471 (17)	1.852 (2)
P1—C11		1.856 (2)
C1—P1—C11	108.78 (11)	105.74 (9)
C1—P1—H1	100 (2)	109.1 (2)
C1—P1—H1 ⁱ /C11—P1—H1	99 (2)	118.4 (2)
Aryl—aryl twist angle	84.39 (10)	94.12 (9)

Symmetry code: (i) $-x + \frac{3}{2}, y, -z + \frac{3}{2}$.

vectors are likely to be accurate. Though some residual density remains, most prominently in the structure of polymorph **II**, there are no peaks greater than 0.5 e \AA^{-3} and they do not appear to be in positions that could correspond to atoms; the largest peak is altogether too close to the P atom ($<1 \text{ \AA}$) and/or in a position that would make little sense in terms of molecular geometry. It is possible that these residual peaks are the result of series termination errors (Fourier ripples).

3. Results and discussion

The two structures of bis(2,3,5,6-tetramethylphenyl)phosphine crystallize in different monoclinic space groups. Polymorph **I** crystallizes in the space group $P2_1/n$, with an asymmetric unit comprising half of the molecule ($Z' = 0.5$). Here the P atom is located on the twofold rotation axis in the structure and the full molecule is generated through this symmetry operation. Polymorph **II** crystallizes in the space group $P2_1/c$, with one whole molecule in the asymmetric unit. In both structures, the proton on the P atom is disordered over two positions, as has been observed previously in similar bis(aryl) secondary phosphine structures (Izod *et al.*, 2017b; Clegg, 2017). Details of the refinements for both structures are presented in Table 1.

Though the bond distances do not differ significantly, the conformations of the molecules in the two polymorphs are somewhat different, as demonstrated by overlaying them (Fig. 2). The conformational variation can be attributed to differences in the geometry about the P atom and the angles between the planes of the aryl rings (Table 2). As polymorph **I** exhibits a wider C—P—C angle than polymorph **II**, this would

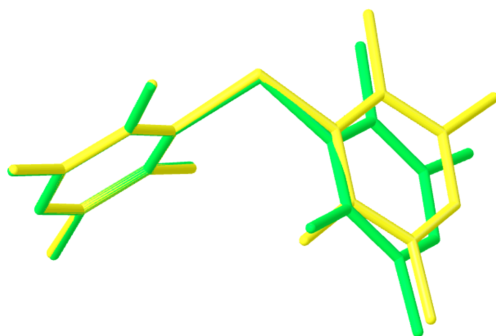


Figure 2
Overlay diagram of polymorphs **I** (yellow) and **II** (green).

Table 3
Intermolecular $\text{Me} \cdots \pi$ interactions (\AA , $^\circ$) in the structure of polymorph.

$D-H \cdots A$	$D \cdots A$	$H \cdots A$	$D-H \cdots A$
C18—H18A \cdots C15 ⁱ	3.694 (4)	2.83 (2)	150 (1)
C19 ⁱ —H19B ⁱ \cdots C15	3.637 (4)	2.88 (2)	136.6 (9)

Symmetry code: (i) $-x + 1, -y + 2, -z + 1$.

suggest that it experiences a greater degree of steric hindrance at the phosphorus centre (Rivard *et al.*, 2007).

The degree of steric pressure on the P atom in bis(aryl)phosphines can also be assessed by the sum of the angles about phosphorus, $\Sigma^\circ\text{P}$ (Boeré & Zhang, 2005). The values measured exceed 300° , with polymorph **I** exhibiting a $\Sigma^\circ\text{P}$ of $318 (2)^\circ$ and the same sum being $333.2 (2)^\circ$ for polymorph **II** (measured for the H atom of highest occupancy). This would seem to contradict the interpretation of the C—P—C bond angles as, according to the $\Sigma^\circ\text{P}$, the P atom in polymorph **II** is under greater steric pressure in spite of its narrower C—P—C angle. Regardless of the trend in these measurements, that there should be such variation within the same molecule demonstrates the effect that polymorphism can potentially have on these compounds. These conformational perturbations are likely the result of the different packing environments and intermolecular interactions in the two solid-state structures.

As is common in the structures of secondary bis(aryl)phosphines, there are no significant contacts involving the H atom on the phosphorus in either structure (Izod *et al.*, 2017b; Bartlett *et al.*, 1987; Clegg, 2017; Rivard *et al.*, 2007; Fleming *et al.*, 2013; Ritch *et al.*, 2014). The lack of structure-directing interactions involving this atom may well be the root of the disorder of the P—H proton manifest in both polymorphs.

The packing in both structures seems to prioritize the minimization of steric interactions as opposed to forming strong structure-directing intermolecular bonds. As such, the packing is best described in terms of the alignment of the aryl rings. The molecules in polymorph **I** stack forming continuous columns along both the crystallographic [100] direction, with P \cdots P distances of *ca* 6.55 \AA (Fig. 3), and along the [010] direction, with an equivalent distance of *ca* 5.99 \AA (the lengths

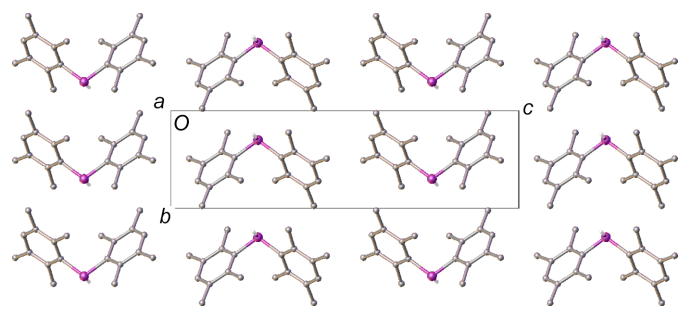


Figure 3
The structure of polymorph **I**, viewed along the [100] direction. Only one orientation of the H atoms bound to phosphorus is shown and the rest have been omitted for clarity.

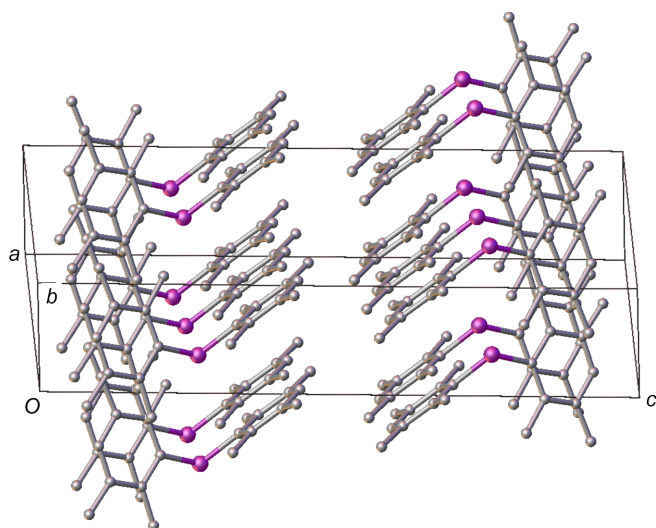


Figure 4
The structure of polymorph **I**, viewed approximately along the $[\bar{1}10]$ direction, showing the direct alignment of the methyl groups hindering close approach of the molecules in this direction. H atoms have been omitted for clarity.

of the respective axes). The rings exhibit similar angles to their respective directions, *ca* 57° in $[100]$ and *ca* 52° in $[010]$.

The distance between the molecules along the columns appears to preclude direct π - π interactions (Avashti *et al.*,

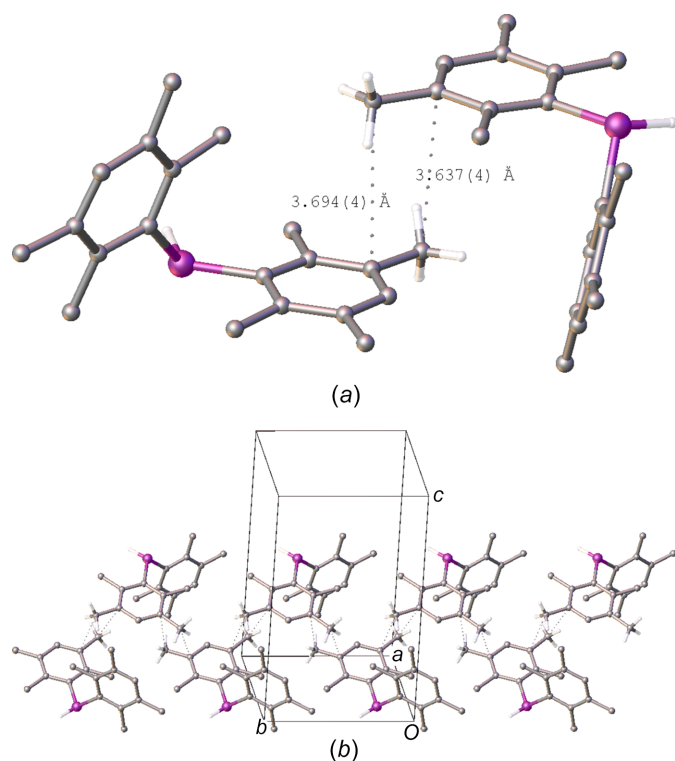


Figure 5
(*a*) A view of the ring motif formed in polymorph **II** of $\text{Me}\cdots\pi$ interactions between two molecules and (*b*) the continuous chain motif formed of these interactions in the $[010]$ direction. Close contacts are depicted as dashed lines and H atoms, with the exception of those bound to phosphorus and the methyl groups involved in intermolecular interactions, have been omitted for clarity.

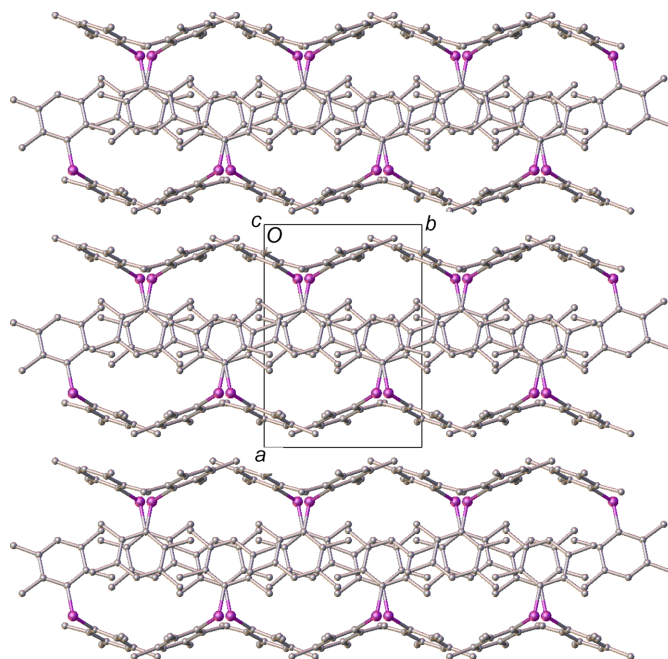


Figure 6
A view of the packing in polymorph **II**, showing the layers coplanar with the crystallographic (100) plane. H atoms have been omitted for clarity.

2014; Brunner *et al.*, 2014). In fact, there do not appear to be any salient intermolecular interactions observed in polymorph **I**. This suggests that the molecules are arranged in such a way as to minimize repulsive contacts rather than form attractive interactions. As a result, all the duryl rings in this structure are orientated coplanar to either the $[110]$ or $[\bar{1}10]$ directions. The orientation of the rings in these directions, with methyl groups directed towards each other in the same plane, further hinders the close approach of the molecules in the structure (Fig. 4).

The packing in the structure of polymorph **II** is markedly different to that in polymorph **I** and much of this can be attributed to the fact that the two aryl rings are crystallographically independent in polymorph **II**. The molecules align along the $[010]$ direction, but the angles of the rings to this direction are shallower than in polymorph **I**; *ca* 28° for one and 0° for the other, where, once again, the methyl groups prevent the close approach of the π systems. Though the arrangement of the rings in the $(\bar{1}02)$ plane, propagating along $[010]$, is reminiscent of a similar arrangement in polymorph **I**, also in the $[010]$ direction, in polymorph **II** the spacing between the molecules in this direction is over 2 \AA longer, with a $\text{P}\cdots\text{P}$ distance of *ca* 8.85 \AA along $[010]$, likely the result of the shallower $\text{P}-\text{C}-\text{P}$ angle.

In contrast to the structure of polymorph **I**, there do appear to be some weak intermolecular interactions in the structure of polymorph **II** in the form of $\text{C}-\text{H}\cdots\text{C}$ contacts between methyl groups and the aromatic rings. Two such contacts, with $\text{C}\cdots\text{C}$ distances $< 3.7 \text{ \AA}$, are observed (Table 3), which can be classified as weak $\text{Me}\cdots\pi$ interactions (Brunner *et al.*, 2014). The two contacts form a ring motif between two of the duryl rings and propagate along the $[010]$ direction, forming a chain

of intermolecular interactions, with each molecule related to the next by the symmetry of the 2_1 screw axis (Fig. 5).

By way of comparison, a similar relationship between the molecules is observed in both the [100] and [010] directions in polymorph **I**; however, in this case, the C \cdots C distances are at least 0.1 Å too long to be considered Me $\cdots\pi$ interactions. Given this, it is possible that the weak but nonetheless attractive interactions observed in polymorph **II** are the root of the shallower C–P–C angle observed in this structure compared to that of polymorph **I**.

Although there are no discernible close contacts between the chains of molecules in polymorph **II**, they appear to pack to form 2D layers coplanar to [100] (Fig. 6). Again, there do not appear to be any significant structure-directing interactions between these layers and the closest centroid–centroid distances between pairs of duryl rings across the layer boundary are *ca* 4.2 Å. As a result, it can be inferred that these rings are orientated simply to minimize steric interactions.

4. Conclusion

Bis(2,3,5,6-tetramethylphenyl)phosphine is the first secondary phosphine known to exhibit polymorphism and is observed to form two different crystalline forms depending on the solvent of crystallization. As structures of these reactive compounds are somewhat rare in the literature, this study expands the sum of structural knowledge of secondary phosphines, as well as revealing aspects of their supramolecular chemistry.

The molecules in each crystal structure vary in terms of their conformation, with the degree of steric pressure on the P atom observed to vary depending on the packing environment. Though polymorph **I** crystallizes with columnar motifs in the [100] and [010] directions, and no significant structure-directing intermolecular interactions, polymorph **II** forms a 2D layered structure with weak Me $\cdots\pi$ interactions, forming a chain motif along the [010] direction.

The study of polymorphism in a secondary phosphine raises some interesting points in terms of the solid-state structures of these molecules. It should be noted that as the same molecule exhibits drastically different values for $\Sigma^\circ\text{P}$, a measure of the steric pressure on the P atom, that this is not an intrinsic molecular property and can be affected by the packing environment. This demonstrates that caution should be exercised when drawing conclusions based on these values, especially in the context of solution-phase calculations.

Acknowledgements

The authors thank the Engineering and Physical Sciences Research Council for the X-ray crystallography facilities.

Conflict of interest

The author declares no competing financial interests.

Funding information

Funding for this research was provided by: Engineering and Physical Sciences Research Council (grant No. EP/F03637X/1).

References

- Avasthi, K., Shukla, L., Kant, R. & Ravikumar, K. (2014). *Acta Cryst. C* **70**, 555–561.
- Bartlett, R. A., Olmstead, M. M., Power, P. P. & Sigel, G. A. (1987). *Inorg. Chem.* **26**, 1941–1946.
- Boeré, R. T. & Zhang, Y. (2005). *J. Organomet. Chem.* **690**, 2651–2657.
- Brunner, H., Tsuno, T., Balázs, G. & Bodensteiner, M. (2014). *J. Org. Chem.* **79**, 11454–11462.
- Clark, R. C. & Reid, J. S. (1995). *Acta Cryst. A* **51**, 887–897.
- Clegg, W. (2017). *CSD Communication* (CCDC 1571091; refcode MEBCOO). CCDC, Cambridge, UK.
- Dolomanov, O. V., Bourhis, L. J., Gildea, R. J., Howard, J. A. K. & Puschmann, H. (2009). *J. Appl. Cryst.* **42**, 339–341.
- Fleming, C. G. E., Slawin, A. M. Z., Athukorala Arachchige, K. S., Randall, R., Bühl, M. & Kilian, P. (2013). *Dalton Trans.* **42**, 1437–1450.
- Groom, C. R., Bruno, I. J., Lightfoot, M. P. & Ward, S. C. (2016). *Acta Cryst. B* **72**, 171–179.
- Izod, K. (2000). *Adv. Inorg. Chem.* **50**, 33–108.
- Izod, K., Evans, P. & Waddell, P. G. (2017a). *Angew. Chem. Int. Ed.* **56**, 5593–5597.
- Izod, K., Evans, P. & Waddell, P. G. (2017b). *Dalton Trans.* **46**, 13824–13834.
- Izod, K., Liu, M., Evans, P., Wills, C., Dixon, C. M., Waddell, P. G. & Probert, M. R. (2022). *Angew. Chem. Int. Ed.* **61**, e202208851.
- Rigaku OD (2015). *CrysAlis PRO*. Rigaku Oxford Diffraction Ltd, Yarnton, Oxfordshire, England.
- Ritch, J. S., Julienne, D., Rybchinski, S. R., Brockman, K. S., Johnson, K. R. D. & Hayes, P. G. (2014). *Dalton Trans.* **43**, 267–276.
- Rivard, E., Sutton, A. D., Fettinger, J. C. & Power, P. P. (2007). *Inorg. Chim. Acta*, **360**, 1278–1286.
- Sheldrick, G. M. (2015a). *Acta Cryst. A* **71**, 3–8.
- Sheldrick, G. M. (2015b). *Acta Cryst. C* **71**, 3–8.

supporting information

Acta Cryst. (2025). C81, 109-113 [https://doi.org/10.1107/S2053229625000555]

Polymorphism in a secondary phosphine

Mo Liu, Keith Izod and Paul G. Waddell

Computing details

Bis(2,3,5,6-tetramethylphenyl)phosphine (kji190001_fa)

Crystal data

$C_{20}H_{27}P$	$F(000) = 324$
$M_r = 298.38$	$D_x = 1.178 \text{ Mg m}^{-3}$
Monoclinic, $P2_1/n$	Cu $K\alpha$ radiation, $\lambda = 1.54184 \text{ \AA}$
$a = 6.5476 (2) \text{ \AA}$	Cell parameters from 4245 reflections
$b = 5.9910 (2) \text{ \AA}$	$\theta = 4.1\text{--}66.4^\circ$
$c = 21.5676 (6) \text{ \AA}$	$\mu = 1.35 \text{ mm}^{-1}$
$\beta = 96.020 (2)^\circ$	$T = 150 \text{ K}$
$V = 841.36 (4) \text{ \AA}^3$	Block, colourless
$Z = 2$	$0.24 \times 0.08 \times 0.06 \text{ mm}$

Data collection

Rigaku Xcalibur Gemini ultra diffractometer with an Atlas detector	$T_{\min} = 0.696$, $T_{\max} = 0.866$
Radiation source: fine-focus sealed X-ray tube, Enhance Ultra (Cu) X-ray Source	11409 measured reflections
Mirror monochromator	1500 independent reflections
Detector resolution: $10.3968 \text{ pixels mm}^{-1}$	1299 reflections with $I > 2\sigma(I)$
ω scans	$R_{\text{int}} = 0.040$
Absorption correction: analytical [CrysAlis PRO (Rigaku OD, 2015), based on expressions derived by Clark & Reid (1995)]	$\theta_{\max} = 66.9^\circ$, $\theta_{\min} = 4.1^\circ$
	$h = -7 \rightarrow 7$
	$k = -7 \rightarrow 7$
	$l = -25 \rightarrow 24$

Refinement

Refinement on F^2	Hydrogen site location: mixed
Least-squares matrix: full	H atoms treated by a mixture of independent and constrained refinement
$R[F^2 > 2\sigma(F^2)] = 0.039$	$w = 1/[\sigma^2(F_o^2) + (0.0665P)^2 + 0.3189P]$
$wR(F^2) = 0.118$	where $P = (F_o^2 + 2F_c^2)/3$
$S = 1.06$	$(\Delta/\sigma)_{\max} = 0.001$
1500 reflections	$\Delta\rho_{\max} = 0.27 \text{ e \AA}^{-3}$
103 parameters	$\Delta\rho_{\min} = -0.24 \text{ e \AA}^{-3}$
0 restraints	
Primary atom site location: dual	

Special details

Geometry. All esds (except the esd in the dihedral angle between two l.s. planes) are estimated using the full covariance matrix. The cell esds are taken into account individually in the estimation of esds in distances, angles and torsion angles; correlations between esds in cell parameters are only used when they are defined by crystal symmetry. An approximate (isotropic) treatment of cell esds is used for estimating esds involving l.s. planes.

Refinement. Single-crystal diffraction was carried out on a Rigaku Xcalibur Atlas Gemini ultra diffractometer using Cu $K\alpha$ radiation ($\lambda = 1.54184 \text{ \AA}$). Data were collected at 150 K using an Oxford Cryosystems CryostreamPlus open-flow N_2 cooling device. Intensities were corrected for absorption using a multifaceted crystal model created by indexing the faces of the crystal for which data were collected (Clark & Reid, 1995). Cell refinement, data collection and data reduction were undertaken via the software *CrysAlis PRO* (Rigaku OD, 2024). Both structures were solved using *SHELXT* (Sheldrick, 2015) and refined by *SHELXL* (Sheldrick, 2008) using the *OLEX2* interface (Dolomanov *et al.*, 2009).

Fractional atomic coordinates and isotropic or equivalent isotropic displacement parameters (\AA^2)

	x	y	z	U_{iso}^*/U_{eq}	Occ. (<1)
P1	0.7500	0.70011 (11)	0.7500	0.0370 (2)	
H1	0.930 (8)	0.760 (8)	0.736 (2)	0.055*	0.5
C1	0.6681 (2)	0.5206 (3)	0.68230 (8)	0.0305 (4)	
C2	0.4837 (3)	0.5804 (3)	0.64606 (8)	0.0334 (4)	
C3	0.4182 (3)	0.4548 (3)	0.59272 (8)	0.0355 (4)	
C4	0.5370 (3)	0.2772 (3)	0.57701 (8)	0.0382 (4)	
H4	0.4904	0.1910	0.5413	0.046*	
C5	0.7214 (3)	0.2184 (3)	0.61090 (8)	0.0345 (4)	
C6	0.7905 (2)	0.3439 (3)	0.66413 (8)	0.0311 (4)	
C7	0.3561 (3)	0.7772 (4)	0.66223 (10)	0.0461 (5)	
H7A	0.2539	0.7281	0.6894	0.069*	
H7B	0.2860	0.8413	0.6239	0.069*	
H7C	0.4453	0.8903	0.6838	0.069*	
C8	0.2213 (3)	0.5095 (4)	0.55258 (9)	0.0465 (5)	
H8A	0.1051	0.4965	0.5775	0.070*	
H8B	0.2028	0.4051	0.5175	0.070*	
H8C	0.2284	0.6623	0.5367	0.070*	
C9	0.8429 (3)	0.0249 (4)	0.58956 (9)	0.0461 (5)	
H9A	0.7649	-0.0477	0.5539	0.069*	
H9B	0.8689	-0.0828	0.6237	0.069*	
H9C	0.9740	0.0791	0.5773	0.069*	
C10	0.9941 (3)	0.2855 (3)	0.70003 (8)	0.0353 (4)	
H10A	1.0520	0.4184	0.7218	0.053*	
H10B	1.0888	0.2315	0.6711	0.053*	
H10C	0.9734	0.1686	0.7305	0.053*	

Atomic displacement parameters (\AA^2)

	U^{11}	U^{22}	U^{33}	U^{12}	U^{13}	U^{23}
P1	0.0399 (4)	0.0324 (4)	0.0362 (4)	0.000	-0.0071 (3)	0.000
C1	0.0282 (8)	0.0338 (9)	0.0288 (8)	-0.0022 (7)	-0.0002 (6)	0.0041 (7)
C2	0.0288 (8)	0.0381 (9)	0.0324 (9)	0.0010 (7)	-0.0003 (7)	0.0066 (7)
C3	0.0276 (8)	0.0485 (11)	0.0294 (9)	-0.0006 (8)	-0.0014 (7)	0.0091 (8)
C4	0.0366 (9)	0.0509 (11)	0.0259 (8)	-0.0027 (8)	-0.0024 (7)	-0.0018 (8)
C5	0.0335 (9)	0.0401 (10)	0.0295 (8)	0.0007 (7)	0.0011 (7)	0.0017 (7)
C6	0.0282 (8)	0.0355 (9)	0.0290 (8)	-0.0011 (7)	0.0004 (7)	0.0056 (7)
C7	0.0369 (10)	0.0486 (11)	0.0506 (11)	0.0103 (9)	-0.0063 (8)	0.0003 (9)
C8	0.0337 (9)	0.0683 (14)	0.0351 (10)	0.0034 (9)	-0.0070 (8)	0.0075 (9)
C9	0.0490 (11)	0.0484 (11)	0.0397 (10)	0.0083 (9)	-0.0010 (8)	-0.0068 (9)

C10	0.0298 (9)	0.0410 (10)	0.0340 (9)	0.0030 (7)	-0.0024 (7)	0.0025 (8)
-----	------------	-------------	------------	------------	-------------	------------

Geometric parameters (Å, °)

P1—H1	1.29 (5)	C6—C10	1.510 (2)
P1—C1 ⁱ	1.8472 (17)	C7—H7A	0.9800
P1—C1	1.8471 (17)	C7—H7B	0.9800
C1—C2	1.414 (2)	C7—H7C	0.9800
C1—C6	1.408 (2)	C8—H8A	0.9800
C2—C3	1.404 (3)	C8—H8B	0.9800
C2—C7	1.507 (3)	C8—H8C	0.9800
C3—C4	1.381 (3)	C9—H9A	0.9800
C3—C8	1.512 (2)	C9—H9B	0.9800
C4—H4	0.9500	C9—H9C	0.9800
C4—C5	1.390 (3)	C10—H10A	0.9800
C5—C6	1.407 (3)	C10—H10B	0.9800
C5—C9	1.505 (3)	C10—H10C	0.9800
C1 ⁱ —P1—H1	98 (2)	C2—C7—H7C	109.5
C1—P1—H1	100 (2)	H7A—C7—H7B	109.5
C1—P1—C1 ⁱ	108.78 (11)	H7A—C7—H7C	109.5
C2—C1—P1	116.72 (13)	H7B—C7—H7C	109.5
C6—C1—P1	122.08 (12)	C3—C8—H8A	109.5
C6—C1—C2	120.98 (16)	C3—C8—H8B	109.5
C1—C2—C7	122.17 (16)	C3—C8—H8C	109.5
C3—C2—C1	119.14 (16)	H8A—C8—H8B	109.5
C3—C2—C7	118.68 (15)	H8A—C8—H8C	109.5
C2—C3—C8	121.47 (17)	H8B—C8—H8C	109.5
C4—C3—C2	118.86 (15)	C5—C9—H9A	109.5
C4—C3—C8	119.67 (17)	C5—C9—H9B	109.5
C3—C4—H4	118.4	C5—C9—H9C	109.5
C3—C4—C5	123.14 (17)	H9A—C9—H9B	109.5
C5—C4—H4	118.4	H9A—C9—H9C	109.5
C4—C5—C6	118.78 (17)	H9B—C9—H9C	109.5
C4—C5—C9	119.49 (17)	C6—C10—H10A	109.5
C6—C5—C9	121.73 (16)	C6—C10—H10B	109.5
C1—C6—C10	121.94 (15)	C6—C10—H10C	109.5
C5—C6—C1	119.01 (15)	H10A—C10—H10B	109.5
C5—C6—C10	119.05 (15)	H10A—C10—H10C	109.5
C2—C7—H7A	109.5	H10B—C10—H10C	109.5
C2—C7—H7B	109.5		

Symmetry code: (i) $-x+3/2, y, -z+3/2$.

Bis(2,3,5,6-tetramethylphenyl)phosphine (kji190003_fa)

Crystal data

$C_{20}H_{27}P$	$F(000) = 648$
$M_r = 298.38$	$D_x = 1.159 \text{ Mg m}^{-3}$
Monoclinic, $P2_1/c$	Cu $K\alpha$ radiation, $\lambda = 1.54184 \text{ \AA}$
$a = 12.8874 (6) \text{ \AA}$	Cell parameters from 3351 reflections
$b = 8.8455 (3) \text{ \AA}$	$\theta = 5.8\text{--}66.7^\circ$
$c = 15.4635 (7) \text{ \AA}$	$\mu = 1.33 \text{ mm}^{-1}$
$\beta = 104.108 (5)^\circ$	$T = 150 \text{ K}$
$V = 1709.61 (13) \text{ \AA}^3$	Block, colourless
$Z = 4$	$0.36 \times 0.14 \times 0.05 \text{ mm}$

Data collection

Rigaku Xcalibur Gemini ultra diffractometer with an Atlas detector	$T_{\min} = 0.746$, $T_{\max} = 0.939$
Radiation source: fine-focus sealed X-ray tube, Enhance Ultra (Cu) X-ray Source	12709 measured reflections
Mirror monochromator	3021 independent reflections
Detector resolution: $10.3968 \text{ pixels mm}^{-1}$	2424 reflections with $I > 2\sigma(I)$
ω scans	$R_{\text{int}} = 0.039$
Absorption correction: analytical [CrysAlis PRO (Rigaku OD, 2015), based on expressions derived by Clark & Reid (1995)]	$\theta_{\max} = 66.8^\circ$, $\theta_{\min} = 3.5^\circ$
	$h = -15 \rightarrow 15$
	$k = -10 \rightarrow 9$
	$l = -18 \rightarrow 18$

Refinement

Refinement on F^2	Hydrogen site location: mixed
Least-squares matrix: full	H atoms treated by a mixture of independent and constrained refinement
$R[F^2 > 2\sigma(F^2)] = 0.047$	$w = 1/[\sigma^2(F_o^2) + (0.0698P)^2 + 0.7357P]$
$wR(F^2) = 0.135$	where $P = (F_o^2 + 2F_c^2)/3$
$S = 1.06$	$(\Delta/\sigma)_{\max} = 0.001$
3021 reflections	$\Delta\rho_{\max} = 0.43 \text{ e \AA}^{-3}$
214 parameters	$\Delta\rho_{\min} = -0.35 \text{ e \AA}^{-3}$
182 restraints	
Primary atom site location: dual	

Special details

Geometry. All esds (except the esd in the dihedral angle between two l.s. planes) are estimated using the full covariance matrix. The cell esds are taken into account individually in the estimation of esds in distances, angles and torsion angles; correlations between esds in cell parameters are only used when they are defined by crystal symmetry. An approximate (isotropic) treatment of cell esds is used for estimating esds involving l.s. planes.

Refinement. The hydrogen atom bound to phosphorous in this structure has been modelled over two positions. The P-H bond lengths were constrained to be similar using the SADI card. To prevent the close contact of one of these disordered hydrogens with an adjacent methyl group, this methyl group was also modelled as disordered over two positions. Single-crystal diffraction was carried out on a Rigaku Xcalibur Atlas Gemini ultra diffractometer using Cu $K\alpha$ radiation ($\lambda = 1.54184 \text{ \AA}$). Data were collected at 150 K using an Oxford Cryosystems CryostreamPlus open-flow N_2 cooling device. Intensities were corrected for absorption using a multifaceted crystal model created by indexing the faces of the crystal for which data were collected (Clark & Reid, 1995). Cell refinement, data collection and data reduction were undertaken via the software *CrysAlis PRO* (Rigaku OD, 2024). Both structures were solved using *SHELXT* (Sheldrick, 2015) and refined by *SHELXL* (Sheldrick, 2008) using the *OLEX2* interface (Dolomanov *et al.*, 2009).

Fractional atomic coordinates and isotropic or equivalent isotropic displacement parameters (\AA^2)

	<i>x</i>	<i>y</i>	<i>z</i>	$U_{\text{iso}}^*/U_{\text{eq}}$	Occ. (<1)
P1	0.75650 (5)	0.71204 (7)	0.50367 (4)	0.0411 (2)	

H1A	0.822 (3)	0.827 (4)	0.527 (3)	0.049*	0.6323
H1B	0.745 (6)	0.639 (7)	0.574 (3)	0.049*	0.3677
C1	0.81783 (16)	0.5738 (2)	0.44111 (15)	0.0357 (5)	
C2	0.82942 (16)	0.6093 (2)	0.35486 (15)	0.0353 (5)	
C3	0.87100 (17)	0.4999 (3)	0.30694 (16)	0.0401 (5)	
C4	0.90209 (18)	0.3610 (3)	0.34647 (17)	0.0431 (5)	
H4	0.9272	0.2876	0.3136	0.052*	
C5	0.89728 (17)	0.3273 (2)	0.43253 (17)	0.0407 (5)	
C6	0.85536 (16)	0.4348 (2)	0.48175 (15)	0.0381 (5)	
C7	0.80033 (19)	0.7628 (3)	0.31418 (16)	0.0422 (5)	
H7A	0.7252	0.7802	0.3072	0.063*	
H7B	0.8168	0.7672	0.2570	0.063*	
H7C	0.8404	0.8389	0.3525	0.063*	
C8	0.8851 (2)	0.5296 (3)	0.21425 (18)	0.0549 (6)	
H8A	0.9130	0.4407	0.1924	0.082*	
H8B	0.9340	0.6121	0.2161	0.082*	
H8C	0.8172	0.5549	0.1753	0.082*	
C9	0.93877 (19)	0.1764 (3)	0.47214 (19)	0.0504 (6)	
H9A	0.8850	0.1278	0.4958	0.076*	
H9B	1.0020	0.1917	0.5191	0.076*	
H9C	0.9557	0.1139	0.4267	0.076*	
C11	0.62051 (16)	0.7494 (2)	0.43286 (14)	0.0327 (4)	
C12	0.55112 (17)	0.6284 (2)	0.39960 (14)	0.0339 (5)	
C13	0.44829 (17)	0.6597 (2)	0.34621 (14)	0.0359 (5)	
C14	0.41651 (17)	0.8083 (3)	0.32953 (14)	0.0373 (5)	
H14	0.3488	0.8279	0.2935	0.045*	
C15	0.48205 (17)	0.9295 (2)	0.36467 (14)	0.0346 (5)	
C16	0.58531 (16)	0.9002 (2)	0.41712 (14)	0.0326 (5)	
C17	0.58273 (19)	0.4660 (2)	0.42098 (17)	0.0423 (5)	
H17A	0.5214	0.4094	0.4271	0.063*	
H17B	0.6372	0.4615	0.4758	0.063*	
H17C	0.6098	0.4237	0.3737	0.063*	
C18	0.37332 (19)	0.5335 (3)	0.30559 (17)	0.0464 (6)	
H18A	0.4081	0.4686	0.2716	0.070*	
H18B	0.3099	0.5754	0.2672	0.070*	
H18C	0.3543	0.4761	0.3521	0.070*	
C19	0.44052 (19)	1.0886 (3)	0.34468 (17)	0.0435 (5)	
H19A	0.3728	1.0857	0.3017	0.065*	
H19B	0.4906	1.1461	0.3211	0.065*	
H19C	0.4318	1.1352	0.3985	0.065*	
C20	0.65494 (19)	1.0335 (2)	0.45548 (16)	0.0416 (5)	
H20A	0.6931	1.0680	0.4131	0.062*	
H20B	0.7051	1.0034	0.5094	0.062*	
H20C	0.6108	1.1138	0.4683	0.062*	
C10A	0.848 (2)	0.404 (3)	0.5765 (8)	0.047 (3)	0.6323
H10A	0.8322	0.4960	0.6033	0.071*	0.6323
H10B	0.9150	0.3641	0.6103	0.071*	0.6323
H10C	0.7923	0.3314	0.5758	0.071*	0.6323

C10B	0.859 (4)	0.384 (5)	0.5759 (14)	0.046 (5)	0.3677
H10D	0.8657	0.4701	0.6143	0.069*	0.3677
H10E	0.9192	0.3178	0.5965	0.069*	0.3677
H10F	0.7943	0.3302	0.5765	0.069*	0.3677

Atomic displacement parameters (\AA^2)

	U^{11}	U^{22}	U^{33}	U^{12}	U^{13}	U^{23}
P1	0.0397 (3)	0.0397 (3)	0.0411 (3)	0.0051 (2)	0.0046 (2)	-0.0048 (2)
C1	0.0302 (10)	0.0325 (10)	0.0424 (11)	0.0001 (8)	0.0050 (8)	0.0008 (9)
C2	0.0294 (10)	0.0320 (10)	0.0429 (11)	-0.0008 (8)	0.0059 (9)	0.0022 (8)
C3	0.0346 (11)	0.0386 (11)	0.0479 (12)	0.0009 (9)	0.0116 (9)	0.0002 (9)
C4	0.0384 (12)	0.0362 (12)	0.0566 (14)	0.0044 (10)	0.0152 (10)	-0.0037 (10)
C5	0.0288 (10)	0.0310 (11)	0.0616 (14)	0.0008 (9)	0.0094 (10)	0.0045 (10)
C6	0.0282 (10)	0.0361 (11)	0.0482 (12)	0.0017 (9)	0.0058 (9)	0.0075 (9)
C7	0.0409 (12)	0.0355 (11)	0.0496 (13)	0.0039 (9)	0.0097 (10)	0.0071 (9)
C8	0.0587 (15)	0.0579 (16)	0.0528 (15)	0.0046 (13)	0.0225 (12)	0.0012 (12)
C9	0.0368 (12)	0.0352 (12)	0.0777 (18)	0.0062 (10)	0.0114 (12)	0.0112 (11)
C11	0.0342 (10)	0.0293 (10)	0.0372 (11)	-0.0006 (8)	0.0135 (8)	-0.0039 (8)
C12	0.0363 (11)	0.0301 (10)	0.0394 (11)	-0.0027 (8)	0.0168 (9)	-0.0030 (8)
C13	0.0376 (11)	0.0352 (11)	0.0386 (11)	-0.0067 (9)	0.0162 (9)	-0.0068 (9)
C14	0.0314 (10)	0.0428 (12)	0.0391 (11)	-0.0008 (9)	0.0115 (9)	-0.0032 (9)
C15	0.0360 (11)	0.0326 (10)	0.0384 (11)	0.0015 (9)	0.0151 (9)	-0.0006 (8)
C16	0.0342 (10)	0.0296 (10)	0.0365 (11)	-0.0017 (8)	0.0132 (8)	-0.0024 (8)
C17	0.0445 (12)	0.0283 (11)	0.0571 (14)	-0.0024 (9)	0.0180 (11)	-0.0011 (10)
C18	0.0428 (13)	0.0443 (13)	0.0549 (14)	-0.0128 (10)	0.0172 (11)	-0.0139 (11)
C19	0.0429 (12)	0.0362 (12)	0.0532 (14)	0.0063 (10)	0.0152 (11)	0.0031 (10)
C20	0.0411 (12)	0.0293 (11)	0.0536 (14)	-0.0030 (9)	0.0102 (10)	-0.0043 (9)
C10A	0.043 (6)	0.042 (6)	0.053 (3)	0.013 (5)	0.006 (3)	0.017 (3)
C10B	0.045 (9)	0.045 (10)	0.050 (5)	0.019 (6)	0.016 (5)	0.009 (4)

Geometric parameters (\AA , $^\circ$)

P1—H1A	1.32 (4)	C12—C13	1.408 (3)
P1—H1B	1.31 (4)	C12—C17	1.508 (3)
P1—C1	1.852 (2)	C13—C14	1.382 (3)
P1—C11	1.856 (2)	C13—C18	1.510 (3)
C1—C2	1.413 (3)	C14—H14	0.9300
C1—C6	1.411 (3)	C14—C15	1.391 (3)
C2—C3	1.402 (3)	C15—C16	1.404 (3)
C2—C7	1.505 (3)	C15—C19	1.511 (3)
C3—C4	1.387 (3)	C16—C20	1.513 (3)
C3—C8	1.511 (3)	C17—H17A	0.9600
C4—H4	0.9300	C17—H17B	0.9600
C4—C5	1.380 (3)	C17—H17C	0.9600
C5—C6	1.406 (3)	C18—H18A	0.9600
C5—C9	1.511 (3)	C18—H18B	0.9600
C6—C10A	1.516 (8)	C18—H18C	0.9600

C6—C10B	1.514 (13)	C19—H19A	0.9600
C7—H7A	0.9600	C19—H19B	0.9600
C7—H7B	0.9600	C19—H19C	0.9600
C7—H7C	0.9600	C20—H20A	0.9600
C8—H8A	0.9600	C20—H20B	0.9600
C8—H8B	0.9600	C20—H20C	0.9600
C8—H8C	0.9600	C10A—H10A	0.9600
C9—H9A	0.9600	C10A—H10B	0.9600
C9—H9B	0.9600	C10A—H10C	0.9600
C9—H9C	0.9600	C10B—H10D	0.9600
C11—C12	1.409 (3)	C10B—H10E	0.9600
C11—C16	1.411 (3)	C10B—H10F	0.9600
C1—P1—H1A	109.1 (18)	C12—C13—C18	120.9 (2)
C1—P1—H1B	105 (3)	C14—C13—C12	119.39 (19)
C1—P1—C11	105.74 (9)	C14—C13—C18	119.7 (2)
C11—P1—H1A	118.4 (18)	C13—C14—H14	118.8
C11—P1—H1B	108 (3)	C13—C14—C15	122.4 (2)
C2—C1—P1	120.22 (16)	C15—C14—H14	118.8
C6—C1—P1	119.09 (17)	C14—C15—C16	118.89 (19)
C6—C1—C2	120.7 (2)	C14—C15—C19	119.2 (2)
C1—C2—C7	121.5 (2)	C16—C15—C19	121.96 (19)
C3—C2—C1	119.18 (19)	C11—C16—C20	122.31 (19)
C3—C2—C7	119.3 (2)	C15—C16—C11	119.61 (19)
C2—C3—C8	122.1 (2)	C15—C16—C20	118.08 (18)
C4—C3—C2	119.0 (2)	C12—C17—H17A	109.5
C4—C3—C8	118.9 (2)	C12—C17—H17B	109.5
C3—C4—H4	118.6	C12—C17—H17C	109.5
C5—C4—C3	122.7 (2)	H17A—C17—H17B	109.5
C5—C4—H4	118.6	H17A—C17—H17C	109.5
C4—C5—C6	119.3 (2)	H17B—C17—H17C	109.5
C4—C5—C9	119.2 (2)	C13—C18—H18A	109.5
C6—C5—C9	121.5 (2)	C13—C18—H18B	109.5
C1—C6—C10A	119.5 (9)	C13—C18—H18C	109.5
C1—C6—C10B	128.0 (15)	H18A—C18—H18B	109.5
C5—C6—C1	118.9 (2)	H18A—C18—H18C	109.5
C5—C6—C10A	121.5 (9)	H18B—C18—H18C	109.5
C5—C6—C10B	113.1 (15)	C15—C19—H19A	109.5
C2—C7—H7A	109.5	C15—C19—H19B	109.5
C2—C7—H7B	109.5	C15—C19—H19C	109.5
C2—C7—H7C	109.5	H19A—C19—H19B	109.5
H7A—C7—H7B	109.5	H19A—C19—H19C	109.5
H7A—C7—H7C	109.5	H19B—C19—H19C	109.5
H7B—C7—H7C	109.5	C16—C20—H20A	109.5
C3—C8—H8A	109.5	C16—C20—H20B	109.5
C3—C8—H8B	109.5	C16—C20—H20C	109.5
C3—C8—H8C	109.5	H20A—C20—H20B	109.5
H8A—C8—H8B	109.5	H20A—C20—H20C	109.5

H8A—C8—H8C	109.5	H20B—C20—H20C	109.5
H8B—C8—H8C	109.5	C6—C10A—H10A	109.5
C5—C9—H9A	109.5	C6—C10A—H10B	109.5
C5—C9—H9B	109.5	C6—C10A—H10C	109.5
C5—C9—H9C	109.5	H10A—C10A—H10B	109.5
H9A—C9—H9B	109.5	H10A—C10A—H10C	109.5
H9A—C9—H9C	109.5	H10B—C10A—H10C	109.5
H9B—C9—H9C	109.5	C6—C10B—H10D	109.5
C12—C11—P1	120.29 (16)	C6—C10B—H10E	109.5
C12—C11—C16	120.43 (19)	C6—C10B—H10F	109.5
C16—C11—P1	119.18 (15)	H10D—C10B—H10E	109.5
C11—C12—C17	122.0 (2)	H10D—C10B—H10F	109.5
C13—C12—C11	119.16 (19)	H10E—C10B—H10F	109.5
C13—C12—C17	118.81 (19)		
